The EMBO Journal Vol. 19 No. 15 pp. 4046–4055, 2000

FIZZ1, a novel cysteine-rich secreted protein associated with pulmonary inflammation, defines a new gene family

Ilona N.Holcomb[1], Rhona C.Kabakoff[2], Betty Chan[2], Thad W.Baker[2], Austin Gurney[3], William Henzel[4], Chris Nelson[4], Henry B.Lowman[5], Barbara D.Wright[1], Nicholas J.Skelton[5], Gretchen D.Frantz[1], Daniel B.Tumas[1], Franklin V.Peale,Jr[1,6], David L.Shelton[7] and Caroline C.Hébert[2]

Departments of [1]Pathology, [2]Immunology, [3]Molecular Biology, [4]Protein Chemistry, [5]Protein Engineering and [7]Neuroscience, Genentech, Inc., 1 DNA Way, South San Francisco, CA 94080, USA

[6]Corresponding author at: Genentech, Inc., Mailstop 72B, 1 DNA Way, South San Francisco, CA 94080-4996, USA
e-mail: fpeale@gene.com

Bronchoalveolar lavage fluid from mice with experimentally induced allergic pulmonary inflammation contains a novel 9.4 kDa cysteine-rich secreted protein, FIZZ1 (found in inflammatory zone). Murine (m) FIZZ1 is the founding member of a new gene family including two other murine genes expressed, respectively, in intestinal crypt epithelium and white adipose tissue, and two related human genes. In control mice, FIZZ1 mRNA and protein expression occur at low levels in a subset of bronchial epithelial cells and in non-neuronal cells adjacent to neurovascular bundles in the peribronchial stroma, and in the wall of the large and small bowel. During allergic pulmonary inflammation, mFIZZ1 expression markedly increases in hypertrophic, hyperplastic bronchial epithelium and appears in type II alveolar pneumocytes. *In vitro*, recombinant mFIZZ1 inhibits the nerve growth factor (NGF)-mediated survival of rat embryonic day 14 dorsal root ganglion (DRG) neurons and NGF-induced CGRP gene expression in adult rat DRG neurons. *In vivo*, FIZZ1 may modulate the function of neurons innervating the bronchial tree, thereby altering the local tissue response to allergic pulmonary inflammation.

Keywords: asthma/bronchial epithelium/colonic epithelium/nerve growth factor (NGF)/sensory neurons

Introduction

Asthma, defined clinically by abnormal, reversible bronchoconstriction in response to a variety of non-specific stimuli, affects 7–10% of children and 5% of adults living in the United States. Approximately two-thirds of cases are caused by allergic sensitivity to environmental antigens, but clinically identical disease can be caused by respiratory infections, inhaled chemical irritants, exercise, emotional stress or cold. Despite the diversity of precipitating factors, the pathological changes in all cases are relatively similar. Interactions between mast cells, eosinophils, lymphocytes and bronchial tissue result in persistent morphological and physiological changes in all layers of the airways. Typically, there is hypertrophy and hyperplasia of the bronchial epithelium, thickening of the basal lamina, hypertrophy of the bronchial submucosal glands with increased mucus production and hypertrophy of bronchial smooth muscle (McFadden and Gilbert, 1992). Most importantly, peribronchial smooth muscle, controlled by sympathetic, parasympathetic and non-adrenergic, non-cholinergic (NANC) inputs, shows increased excitability resulting in inappropriate but reversible constriction of the airways (airway hyperresponsiveness; AHR), the hallmark clinical presentation of asthma (Barnes, 1996).

By correlating findings in human asthma with those in experimental animal models, a variety of small molecule and protein mediators, including histamine, bradykinin, prostaglandins, leukotrienes and cytokines have been implicated in promoting allergic inflammation and bronchoconstriction. These molecules may be released from inflammatory cells, nerve terminals or respiratory epithelial cells, and may promote AHR in at least four ways: (i) by amplifying the inflammatory process; (ii) by damaging the respiratory epithelium, thereby increasing irritant access to sensory nerve endings (Davies *et al.*, 1993); (iii) by lowering the threshold for vagal afferent sensory fiber stimulation (Spina *et al*., 1998); or (iv) by increasing responsiveness of bronchial smooth muscle cells to efferent stimulation (Braun *et al*., 1998).

Nerve growth factor (NGF), well known for its role as a sympathetic and sensory nerve growth factor, has been shown to have additional activities both within and outside the nervous system. Of particular relevance to the pathophysiology of asthma, NGF induces acute changes in the excitability of peptidergic sensory neurons (Shu and Mendell, 1999), longer term changes in levels of bioactive peptides such as substance P and calcitonin gene-related peptide (CGRP; Lindsay and Harmar, 1989; Lindsay *et al*., 1989), and changes in the neuronal expression of receptors for bradykinin (Petersen *et al*., 1998). NGF is among the mediators released from mast cells during allergic inflammation, and NGF stimulation of mast cells results in degranulation, potentially amplifying the inflammatory reaction. Elevated serum NGF has been reported in human patients with asthma (Bonini *et al*., 1996). NGF is elevated in serum and bronchoalveolar lavage fluid (BALF) from mice with experimentally induced asthma, and this elevation is correlated with increased bronchial smooth muscle hyperresponsiveness (Braun *et al*., 1998).

In order to identify additional molecules associated with allergic inflammation and AHR, we screened for novel secreted proteins expressed in murine ovalbumin (OVA)-induced asthma. This model reproduces the

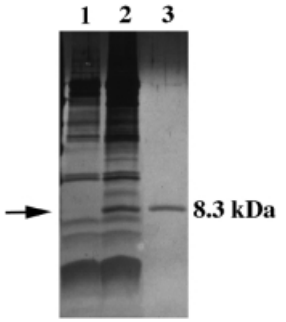

Fig. 1. SDS–acrylamide gel analysis of BALF. Equal volumes (10 µl) of BALF from control mice and BALF obtained from mice with OVA-induced allergic pulmonary inflammation were analyzed under reducing conditions by SDS–PAGE on a Tricine-buffered 16% acrylamide gel. BALF from mice with allergic pulmonary inflammation (lane 2) contains a unique band, co-migrating with an 8.3 kDa molecular weight marker (IL-8, 50 ng, lane 3), which is not present in BALF from control mice (lane 1).

perivascular and peribronchial inflammation, bronchial epithelial hypertrophy and increased mucus production described in human asthma (Blyth *et al*., 1996), making it appropriate for identification of key cellular and biochemical components of the disease state. Here we describe a new gene family, one member of which encodes a protein whose expression *in vivo* and function *in vitro* implicate the molecule as a possible mediator of neuronal function and airway hyperreactivity.

Results

Identification of the FIZZ gene family

SDS–acrylamide gel analysis of BALF collected from mice with OVA-induced pulmonary inflammation revealed a band, co-migrating with an 8.3 kDa marker protein, that was not present in control BALF (Figure 1). The apparent abundance of protein in this band did not correlate with BALF serum albumin concentration as assessed by ELISA (data not shown), indicating that the protein was not simply a component of plasma that had leaked into the alveolar airspace. Concentrations of this protein in the BALF, estimated by comparison with the marker protein, were as high as 0.5–0.75 µM (~5 µg/ml). Microsequencing of the isolated protein allowed the subsequent isolation of a 536 bp cDNA from normal mouse lung. Named FIZZ1 (found in inflammatory zone), the sequence encodes 111 amino acids with an N-terminal signal peptide (amino acids 1–23) and a C-terminal cysteine-rich domain (Figure 2A). The predicted molecular weight and pI of the secreted form of the protein are 9431 Da and 4.83, respectively.

Nucleotide homology searches of the DDBJ/EMBL/GenBank database identified two additional mouse genes and two human genes with homology to murine (m) FIZZ1 (Figure 2A). The relative amino acid homology of various FIZZ family members to each other is illustrated in Figure 2B. All five genes encode proteins with 105–114 amino acids containing signal peptide sequences 10–23 amino acids long, with 10 cysteine residues in the C-terminus having identical spacing [$^{1}CX_{11}{}^{2}CX_{8}$-$^{3}CX^{4}CX_{3}{}^{5}CX_{10}{}^{6}CX^{7}CX^{8}CX_{9}{}^{9}C^{10}C$]. Three of the 10 C-terminal cysteines are embedded within two highly

A

```
mFIZZ1 1 -MKTTTCSLLICISLLQLMVPVNTDETIEIIVENKVKELLANPANYPSTV
mFIZZ2 1 -MKPTLCFLFILVSLFPLIVPGNAQCSFESLVDQRIKEALSRQE------
mFIZZ3 1 MKNLSFPLLFLFFLVPELLGSSMPLCPIDEAIDKKIKQDFNSLFPN-AIK
hFIZZ1 1 -MGPSSCLLLILIPLLQLINPGSTQCSLDSVMDKKIKDVLNSLEYSPSPI
hFIZZ3 1 ----MKALCLLLLPVLGLLVSSKTLCSMEEAINERIQEVAGSLIFR-AIS

mFIZZ1 50 TKTLSCTSVKTMNRWASCPAGMTATGCACGFACGSWEIQSGDTCNCLCLL
mFIZZ2 44 PKTISCTSVTSSGRLASCPAGMVVTGCACGYGCGSWDIRNGNTCHCQCSV
mFIZZ3 50 NIGLNCWTVSSRGKLASCPEGTAVLSCSCGSACGSWDIREEKVCHCQCAR
hFIZZ1 50 SKKLSCASVKSQGRPSSCPAGMAVTGCACGYGCGSWDVQLETTCHCQCSV
hFIZZ3 46 SIGLECQSVTSRGDLATCPRGFAVTGCTCGSACGSWDVRAETTCHCQCAG
Cons.          C  V        CP G     C CG  CGSW       CHC C

mFIZZ1 100 VDWTTARCCQLS
mFIZZ2  94 MDWASARCCRMA
mFIZZ3 100 IDWTAARCCKLQVAS
hFIZZ1 100 VDWTTARCCHLT
hFIZZ3  96 MDWTGARCCRVQP
Cons.       DW  ARCC
```

B

	mF1	mF2	mF3	hF1	hF3
mF1		51%	29%	50%	33%
mF2	66%		37%	59%	43%
mF3	44%	56%		42%	53%
hF1	67%	75%	54%		47%
hF3	46%	59%	64%	61%	

Fig. 2. Sequences of the FIZZ protein family. (**A**) The amino acid sequences of murine and human FIZZ proteins. The consensus sequence (Cons.) indicates the position of the conserved residues. Underlined residues represent predicted signal peptide sequences. The corresponding nucleotide sequences are entered in the DDBJ/EMBL/GenBank databases under the following accession Nos: mFIZZ1, AF205951; mFIZZ2, EST AA245405; mFIZZ3, EST W42069; hFIZZ1, EST AA524300; hFIZZ3, AF205952. (**B**) Amino acid identity (upper right) and homology (lower left) for the five members of the FIZZ gene family (based on PAM250 matrix).

conserved motifs, (A/G)^{5}CGSW(D/E)(I/V) and DW(A/T)XAR^{9}C^{10}C. With the exception of mFIZZ1, all family members have an additional cysteine in the N-terminal domain of the processed form of the protein. The FIZZ proteins lack significant homology to any proteins outside the family, as determined by BLASTP (Altschul *et al*., 1990, 1997), and HMMER 2.1.1 Pfam software (Bateman *et al*., 1999). The nearest Pfam match was to cysteine knot proteins, although the degree of homology was very low (E-values = 22, 11 and 41 for mFIZZ-1, -2 and -3, respectively). Secondary structure prediction indicates that the processed form of the mFIZZ1 protein may contain a helix at the N-terminus (residues Ile6 to Ala17). Examination of the mFIZZ1 amino acid sequence with the threading package ProCyon (Flöckner *et al*., 1997) indicated a poor quality of the match between mFIZZ1 and cysteine knot proteins including NGF, neurotrophin 3 (NT3), brain-derived neurotrophin factor (BDNF), transforming growth factor-β, glial cell line-derived neurotrophic factor (GDNF) and platelet-derived growth factor, consistent with the large E-value given by the Pfam homology search. In all cases, secondary structure elements or locations of cysteine residues were not compatible with the mFIZZ1 sequence. However, the

epidermal growth factor (EGF) fold gave high scores in both the 'pair/surface'- and 'sequence'-based potentials.

Tissue expression of FIZZ genes

Northern blot analysis of adult mouse tissues using an oligonucleotide probe complementary to mFIZZ1 shows expression of a single 750–800 base mRNA primarily in the lung, with ~10-fold lower levels detectable in heart and skeletal muscle (Figure 3). Adult mouse multi-tissue northern blots hybridized with mFIZZ3-specific probes revealed expression at low levels in many organs (data not shown). Recent DDBJ/EMBL/GenBank expressed sequence tag (EST) entries with homology to the various FIZZ genes are as follows: mFIZZ1, AA945994 (rat lung) and AA712003 (mouse mammary gland); mFIZZ2, AA711012 (mouse colon); mFIZZ3, AI746650 (mouse kidney) and AA796118 (mammary gland); human (h) FIZZ1, AI732383 (colon cancer); hFIZZ3, AA311223 (Jurkat T cells).

Expression analysis by in situ hybridization and immunohistochemistry

To characterize the cell type-specific expression of mFIZZ1 in detail, we examined normal and inflamed murine lungs by *in situ* hybridization and immunohistochemistry. In control adult lung, mFIZZ1 mRNA was expressed at low levels in the large airways in small discrete clusters of epithelial cells (Figure 4A, C and E), and in scattered isolated cells in the peribronchiolar stroma (Figure 4G and I). Consistent with the BALF analysis, expression of mFIZZ1 mRNA in lungs with OVA-induced allergic inflammation was markedly increased, with widespread uniform expression in the bronchial mucosal epithelial cells (Figure 4B, D and F). Additionally, in inflamed but not control lungs, mFIZZ1 message was present throughout the lung in scattered cells associated with the alveolar wall, consistent with type II pneumocytes; significantly, no signal was seen in alveolar macrophages (Figure 4H and J).

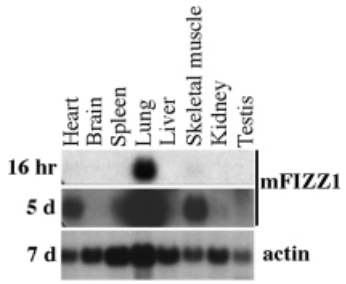

Fig. 3. mFIZZ1 northern blot. A Clontech adult mouse multiple tissue northern blot was probed with an oligonucleotide corresponding to nucleotides 176–225 of the full-length mFIZZ1 sequence, and exposed for 16 h or 5 days as shown. The same blot, stripped and reprobed with an oligonucleotide for β-actin, and exposed for 7 days, is shown at the bottom of the figure.

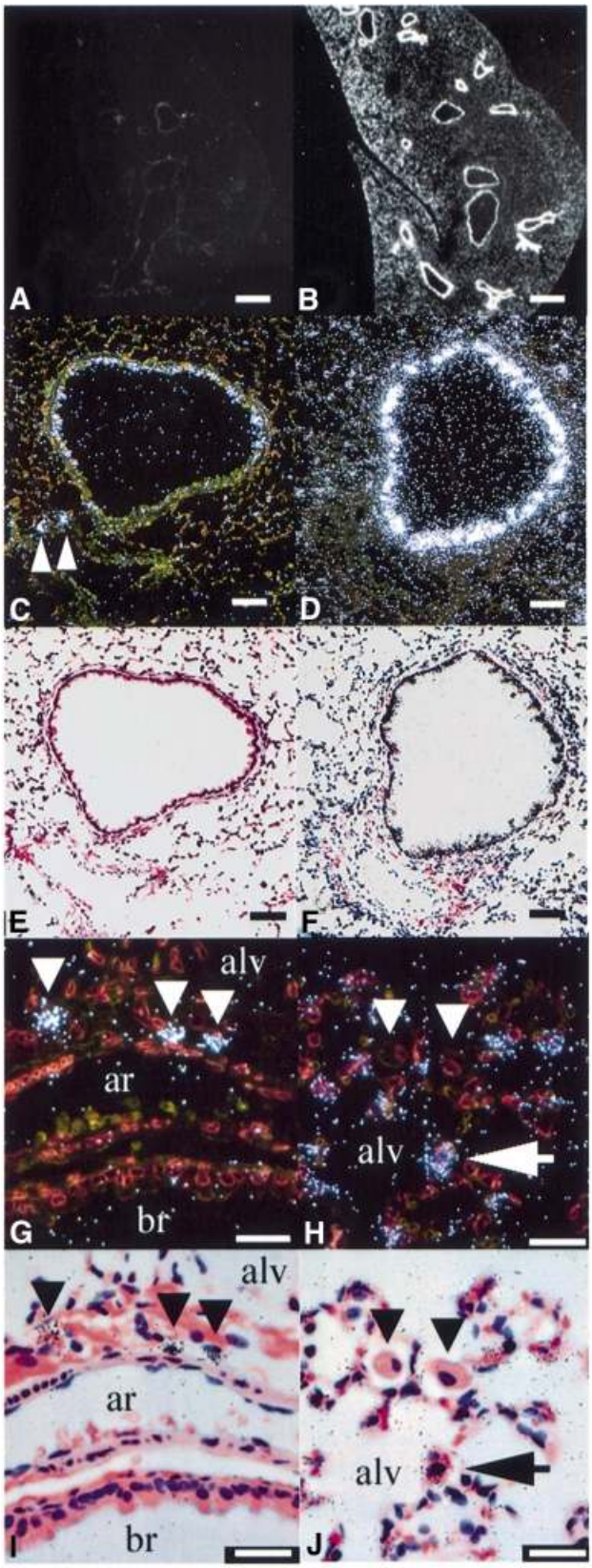

Fig. 4. *In situ* hybridization of mFIZZ 1 in adult mouse lung. A ^{33}P-labeled mFIZZ1 riboprobe detected patchy expression in bronchial epithelium of control (OVA-challenged, non-immunized mouse) lung after a 4-week exposure (**A**, **C** and **E**). In inflamed lung, a 2-week exposure with the same probe detected diffuse strong expression in bronchial epithelium (**B**, **D** and **F**) and type II pneumocytes (arrows, H and J), while alveolar macrophages (arrowheads, H and J) were negative. Murine FIZZ1 expression was also present in discrete cells in neurovascular bundles in peribronchial interstitium (arrowheads, C, G and I). Dark-field images: A–D, G and H. Corresponding bright-field images: E, F, I and J. Scale bars represent 500 μm (A and B), 50 μm (C–F) or 25 μm (G–J). ar, artery; br, bronchiole; alv, alveolar space.

Polyclonal rabbit antiserum to mFIZZ1 was generated against a peptide derived from the N-terminal helical domain, a portion of the protein sharing little homology with other members of the FIZZ family. Western blots (Figure 5) of inflamed lung BALF, resolved under reducing conditions and probed with mFIZZ1 antiserum, detected a single band consistent with mFIZZ1 (lane 2) while pre-immune serum did not detect any specific proteins (lane 1). Whole-lung homogenates from animals with allergic inflammation revealed a similar band under reducing conditions (lane 3). However, under non-reducing conditions, two additional bands were detected, one migrating only slightly more slowly than mFIZZ1, another migrating with an apparent size of 25–30 kDa (lane 4).

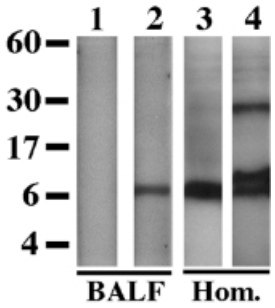

Fig. 5. Western blot analysis of BALF and lung homogenates from mice with allergic pulmonary inflammation. Lane 1, BALF sample resolved under reducing conditions and analyzed with pre-immune serum; lane 2, BALF sample resolved under reducing conditions and analyzed with a rabbit anti-FIZZ1 peptide antiserum. Whole-lung homogenate (Hom.) resolved under reducing (lane 3) or non-reducing conditions (lane 4) and analyzed with the same rabbit antiserum. The migration of molecular size markers (kDa) is indicated on the left.

Immunohistochemistry using the same polyclonal antiserum confirmed the *in situ* hybridization expression results. Limited patchy FIZZ1 protein expression was observed in control bronchial mucosa (Figure 6A and C), whereas inflamed mucosa showed uniform high protein levels (Figure 6B). In alveoli of the inflamed lung, but not in the control lung, scattered plump alveolar epithelial cells, consistent with type II pneumocytes, were strongly positive for FIZZ1 protein (Figure 6D). Alveolar macrophages and many tissue components in the inflamed lungs were weakly positive by immunohistochemistry. Enhanced expression of FIZZ1 in inflamed lung tissue was not restricted to the ovalbumin model: similar changes were seen in a second allergic inflammation model that

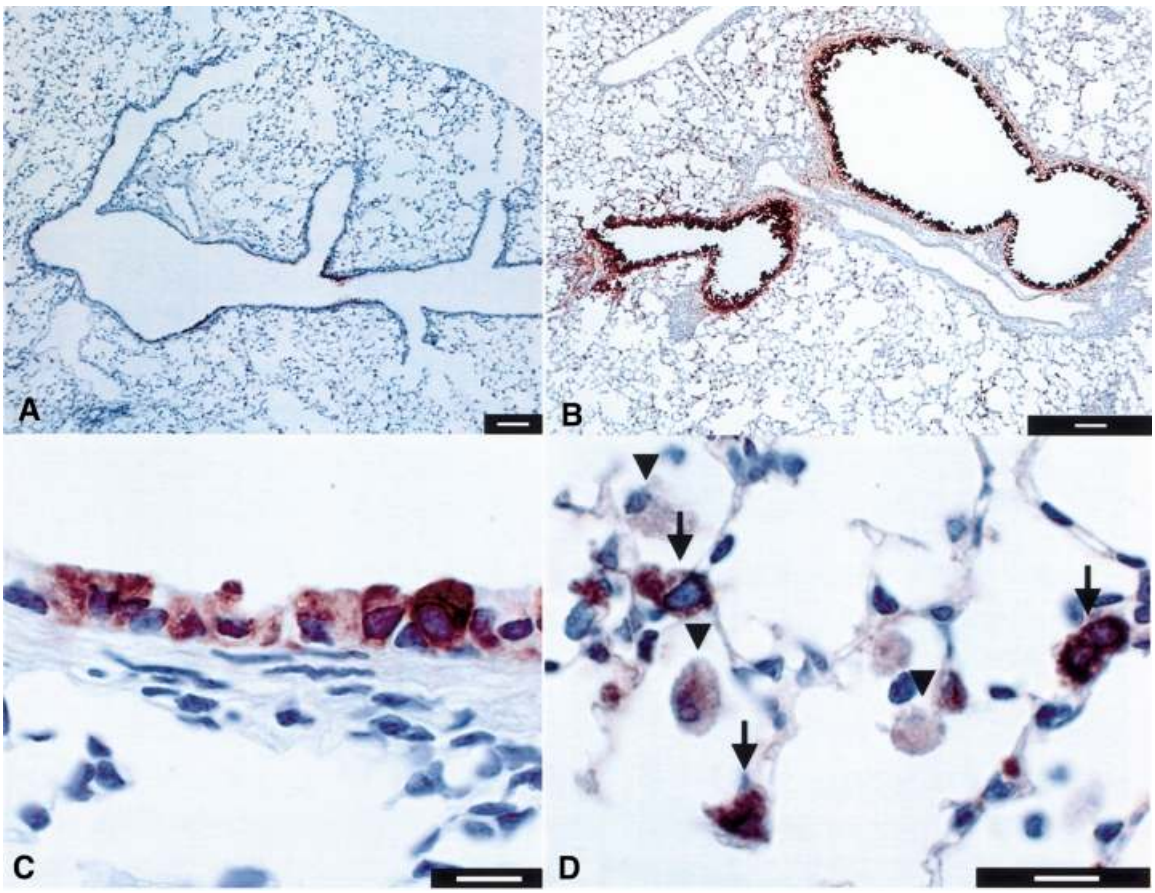

Fig. 6. Immunohistochemical detection of mFIZZ1 protein in inflamed and control lung. (**A** and **C**) Murine FIZZ1 expression in control (OVA-challenged, non-immunized mouse) lung is limited to small patches of bronchial epithelial cells. (**B** and **D**) In the inflamed lungs of immunized, OVA-challenged mice, mFIZZ1 protein expression in bronchial epithelium is both more diffuse and more intense. In addition, expression is seen in alveolar epithelial cells with granular cytoplasm, consistent with type II pneumocytes (arrows, D). Alveolar macrophages (arrrowheads, D) and stromal cellular components stain reproducibly, but weakly with anti-FIZZ antibody, despite being negative for FIZZ mRNA by *in situ* hybridization (Figure 4H and J). Scale bars represent 100 μm (A and B), 10 μm (C) or 25 μm (D).

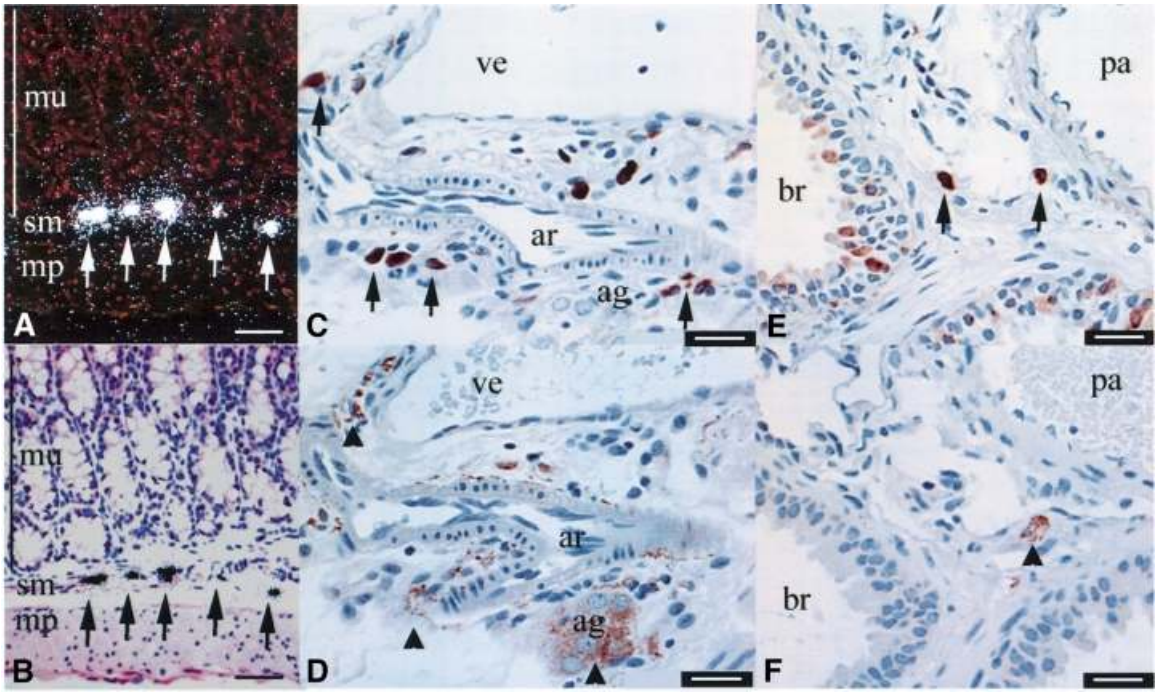

Fig. 7. Expression of mFIZZ1 mRNA in colonic submucosal and peribronchial neurovascular bundles. (**A** and **B**) *In situ* hybridization of mFIZZ1 in colon shows strong expression in discrete cells (arrows) in the submucosa after a 4-week exposure. (C–F) Immunohistochemistry of FIZZ1 (**C** and **E**) and PGP9.5 (**D** and **F**) in serial sections of colonic submucosal (C and D) and peribronchial (E and F) tissue. mFIZZ1-positive cells (arrows) are adjacent to neuronal cell bodies and fibers (arrowheads). Similar results were obtained with antibodies to S-100 and NSE (not shown). Scale bars represent 50 μm (A and B) or 25 μm (C–F). mu, mucosa; sm, submucosa; mp, muscularis propria; ve, venule; ar, arteriole; ag, autonomic ganglion; br, bronchiole; pa, pulmonary artery.

utilized dust mite extract as allergen and which induced similar bronchial epithelial pathology (data not shown).

We examined other tissues for mFIZZ1 mRNA and protein expression. FIZZ1 transcripts and protein were seen in discrete cells adjacent to neurovascular bundles, primarily in the submucosa of the large intestine (Figure 7A–C), and throughout the small bowel wall (not shown). In the colon, mFIZZ1-expressing cells were most often located adjacent to cells expressing neuronal and Schwann cell markers including protein gene product 9.5 (PGP9.5), neuron-specific enolase (NSE) and S-100 (Figure 7D). Occasional mFIZZ1-positive cells were seen in the muscularis propria of the large bowel, generally associated with neurovascular bundles, but no mFIZZ1-positive cells were specifically associated with Auerbach's plexus. Similar cells in the peribronchial stroma (Figures 4G, I and 7E) were adjacent to PGP9.5-positive neurons (Figure 7F). Scattered mFIZZ1-positive cells were noted in mammary gland subcutaneous tissue, in the heart and mediastinum (not shown). There was no epidermal expression of mFIZZ1.

Strong expression of mFIZZ2 mRNA was found in the adult colon in the mucosal crypt epithelial cells; expression was highest in the lower one-half to one-third of the crypt and diminished in the more superficial epithelium (Figure 8A and B). Murine FIZZ2 expression was segmental: *in situ* hybridization using histological sections of 'jelly-rolled' bowel showed positive signal in contiguous regions ~2 cm long alternating with segments of approximately the same length having no detectable expression (Figure 8C and D). In the small bowel, mFIZZ2 was also expressed more highly in the crypts than in the villi (not shown). All other tissues examined were negative.

Murine FIZZ3 mRNA was expressed exclusively in white adipose tissue in a variety of organs (Figure 8E–H). All other tissues, including brown adipose tissue, were negative. The tissue-specific expression patterns of mFIZZ-1, -2 and -3 are summarized in Table I.

Functional studies

Allergic pulmonary inflammation is associated with infiltration of inflammatory cells into the peribronchial tissue, transmigration of inflammatory cells into the airways, increased bronchial secretions and enhanced airway smooth muscle reactivity. Because the expression of mFIZZ1 was significantly upregulated in allergic inflammation *in vivo*, we asked whether the molecule could modify related biological responses *in vitro*. Murine FIZZ1 had no detectable inhibitory activity in assays to measure human neutrophil elastase, trypsin, chymotrypsin or cathepsin G activity (data not shown).

Because mFIZZ1 is expressed by cells intimately associated with submucosal bronchial nerves, we asked whether there was a relationship between mFIZZ1 and NGF activity. We first examined the ability of mFIZZ1 to affect the NGF-induced survival of rat embryonic day (E) 14 dorsal root ganglion (DRG) neurons, the majority of which require NGF for survival *in vitro* and *in vivo* at this age. In agreement with previous results (Levi-Montalcini and Angeletti, 1963), addition of NGF to cultures resulted in increased neuronal survival after 3 days. Recombinant mFIZZ1-his, added to cultures at a concentration equivalent to that found in BALF (4 μg/ml), significantly

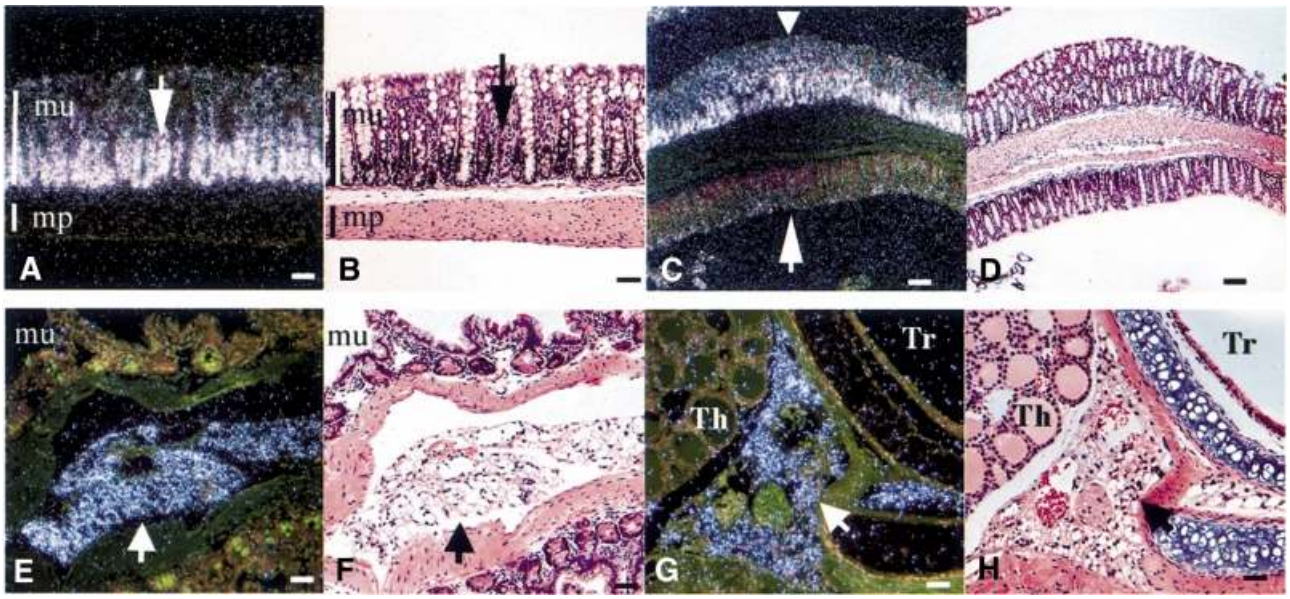

Fig. 8. Expression of mFIZZ2 and mFIZZ3 mRNA. (**A**–**D**) *In situ* hybridization of mFIZZ2 to a section of colon shows strong signal in crypt epithelium after a 2-week exposure. In (C and D), the 'jelly roll' orientation of the colon has artificially brought two segments of colon back-to-back; one segment (arrowhead) is intensely positive for FIZZ2 expression, while the other segment (arrow), several centimeters from the first, is negative. (**E** and **F**) *In situ* hybridization of mFIZZ3 to small bowel and mesentery (4-week exposure). Expression is limited to adipose tissue (arrow) in mesentery. (**G** and **H**) *In situ* hybridization of mFIZZ3 to peritracheal tissue (4-week exposure); expression is limited to adipose tissue (arrow) adjacent to thyroid gland (Th) and trachea (Tr). Dark-field images: A, C, E and G. Corresponding bright-field images: B, D, F and H. Scale bars represent 35 μm (A, B and E–H) or 100 μm (C and D). mu, mucosa; mp, muscularis propria.

Table I. mFIZZ expression summary

Gene	Tissue	Expression pattern
mFIZZ1	normal lung	scattered bronchial epithelial cells; peribronchial stromal cells adjacent to nerves
	inflamed lung	most bronchial epithelial cells; type II pneumocytes
	small, large intestine	submucosal cells adjacent to nerves
	mammary gland	scattered cells in subcutaneous tissue
mFIZZ2	small, large intestine	crypt epithelium
mFIZZ3	white adipose tissue	diffuse expression

inhibited the NGF-induced survival (Figure 9A) without inducing toxicity in non-neuronal cells (not shown).

To rule out the possibility that mFIZZ1-his is selectively toxic to neurons, we took advantage of the fact that adult DRG neurons no longer require NGF for their survival, but do still respond to NGF by induction of CGRP (Lindsay and Harmar, 1989; Horton *et al*., 1998). In agreement with previous work, addition of NGF to cultures of adult DRG neurons did not change the number of surviving neurons as measured by the number of NeuN-positive cells, nor did it change the number of CGRP-positive cells (not shown). However, NGF dramatically increased the CGRP content of adult DRG neurons (Figure 9B). Addition of mFIZZ1-his to these cultures had no effect on neuron survival, nor on the number of CGRP-positive neurons (not shown), ruling out non-specific toxic effects. However, mFIZZ1-his did inhibit, in a dose-dependent fashion, the NGF-mediated increase in neuronal CGRP content (Figure 9B).

To explore the mechanism of this inhibition, we asked if mFIZZ1 inhibited the binding of NGF to its signal transducing receptor, trkA. We examined the effect of mFIZZ1 on NGF binding utilizing a cell-free system of the cloned trkA receptor bound to ELISA plates. This system accurately replicates the affinity and selectivity of the various trk receptors for their natural ligands (Shelton *et al*., 1995). Inclusion of mFIZZ1 in the binding experiments resulted in no change in NGF binding at any concentration tested (D.L.Shelton, data not shown). In order to test for direct interactions between mFIZZ1 and either trkA or NGF, we coupled mFIZZ1, NGF, trkA–IgG or an irrelevant IgG to a surface plasmon resonance (SPR) biosensor chip. Soluble mFIZZ1 showed significant but weak association with immobilized mFIZZ1 (Figure 10A). Soluble mFIZZ1 also interacted detectably with surfaces coupled with NGF, trkA–IgG or the irrelevant IgG, but was eluted rapidly by the control buffer lacking protein. On the other hand, while soluble NGF showed no net binding to immobilized mFIZZ1 or NGF, it did associate, as expected, with surface-bound trkA–IgG with high affinity, deduced from a slow dissociation rate (Figure 10B). Soluble trkA–IgG showed no binding to immobilized mFIZZ1, trkA–IgG or NGF (data not shown), suggesting that NGF immobilized in this manner is sterically hindered from binding to trkA–IgG. In the SPR assay, we therefore observed only transient weak association of soluble mFIZZ1 with immobilized NGF, trkA and

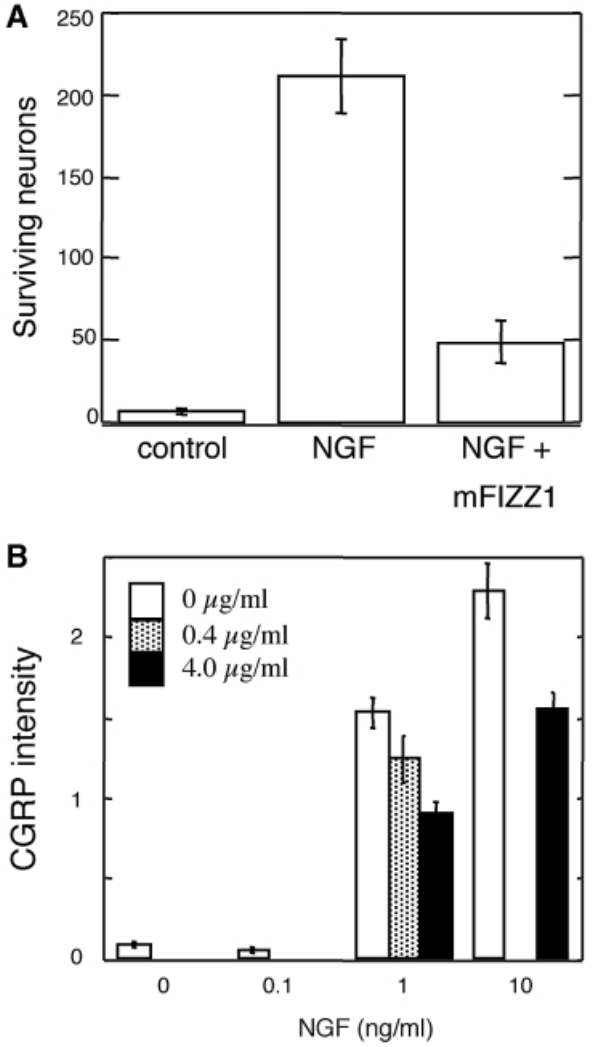

Fig. 9. FIZZ1 inhibits NGF-mediated neuronal survival and gene expression. (**A**) Surviving rat E14 DRG neurons were counted after 3 days in culture. Recombinant mFIZZ1 at 4 μg/ml inhibited neuronal survival without inducing non-neuronal cell toxicity. (**B**) NGF induces higher levels of CGRP immunoreactivity in neurons, and mFIZZ1 inhibits the NGF-induced increase in CGRP content. Open bars, no mFIZZ1; hatched bars, 0.4 μg/ml (~40 nM) mFIZZ1; solid bars, 4 μg/ml (~0.4 μM) mFIZZ1. mFIZZ1 at 4 μg/ml inhibits the increase in CGRP induced by 1 ng/ml NGF (p <0.002) or 10 ng/ml NGF (p <0.01).

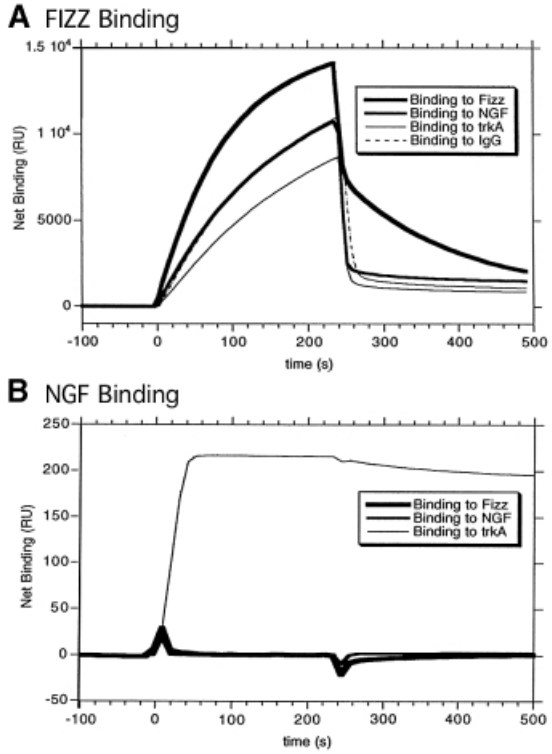

Fig. 10. SPR biosensor measurements of protein–protein binding interactions. mFizz1, NGF, trkA–IgG or an irrelevant IgG was immobilized on a biosensor chip. At time 0, mFizz1 (**A**) or NGF (**B**), each at 0.1 mg/ml, was injected and the response on all four immobilized proteins was recorded. The total response is shown in (A) whereas the net response (RU observed minus RU observed with the irrelevant IgG) is shown in (B).

irrelevant IgG, and no association of immobilized mFIZZ-1 with either soluble trkA or NGF. These results, together with normal trkA–NGF interaction in the presence of mFIZZ1 protein (see above), are consistent with NGF and mFIZZ1 acting through independent mechanisms to affect neuronal function. To our knowledge, this is the first report of a naturally occurring antagonist of a neurotrophin.

Discussion

We describe here three murine genes and two human homologs, which together compose a novel gene family. Each encoded protein has an N-terminal signal peptide, a processed N-terminal domain of 28–44 residues having only limited homology among the family and a well-conserved cysteine-rich C-terminal domain of 57–60 residues with little primary amino acid homology to any known proteins. The predicted tertiary structure of the C-terminus of mFIZZ1 is consistent with an EGF-like fold, although the actual three-dimensional conformation of the protein remains to be described.

The murine FIZZ genes are expressed in distinct tissue-specific patterns, implying divergent biological activities. Murine FIZZ2 is found exclusively in the actively replicating crypt epithelium of the colon and small bowel. The pattern of mFIZZ2 gene expression along the length of the colon shows intriguing segmental variation. To our knowledge, this is the first description of such a pattern in the intestinal epithelium. Murine FIZZ3 is expressed uniquely in white adipose tissue throughout the body. We observed expression specifically in limbs, subcutaneous tissue, mesentery and the mediastinum. This pattern correlates well with northern blot data showing low-level expression in many tissues, when one accounts for the fact that adipose tissue intimately associated with specific organs is not completely removed during routine tissue collection.

Murine FIZZ1 is expressed in at least two tissues: in the lung epithelium and in non-neuronal cells adjacent to neurons, particularly in the submucosa of the gut and in peribronchial stroma. In the lung epithelium, mFIZZ1 expression is specific to two cell types: bronchial mucosal epithelial cells and type II alveolar pneumocytes. While low-level expression is seen in scattered bronchial

epithelial cells in control lungs, increased bronchial epithelial expression and type II pneumocyte expression are seen only in lungs with allergen-induced inflammation. These data suggest that mFIZZ1 may have a role in respiratory epithelial cell maintenance and response to injury. Murine FIZZ1 protein levels measured in BALF (a saline-diluted sample of airway secretions) were very high, as much as 5 μg/ml; the concentration of mFIZZ1 protein in undiluted airway secretions would be higher still. *In vitro* assays of mFIZZ1 function showed significant effects on DRG survival and gene expression at only 0.4 μg/ml, more than an order of magnitude below the levels measured in BALF.

Discrete spindle-shaped cells adjacent to neurovascular bundles in the lung and bowel submucosa expressed mFIZZ1 mRNA and protein. These cells were not identified by neuronal or glial markers (PGP9.5, NSE, S-100) but were adjacent to both neuronal cell bodies and fibers. The intimate association of these cell types suggests a functional relationship. *In vitro* assays show that mFIZZ1 selectively inhibits NGF-mediated embryonic DRG neuron survival and inhibits NGF-induced modulation of gene expression in adult sensory DRG neurons, decreasing CGRP gene expression. Since an *in vitro* trkA receptor binding assay and SPR measurements indicated no specific interaction between mFIZZ1 and NGF or trkA, the *in vivo* effects of mFIZZ1 may be indirect, acting through a separate receptor signaling system in NGF-responsive cells. Alternatively, FIZZ1 may be acting in the DRG culture system in a paracrine fashion on glial cells adjacent to NGF-responsive neurons. In either case, the data support the hypothesis that mFIZZ1 modulates gene expression in peripheral sensory neurons innervating the bronchial tree. If the effect of mFIZZ1 on CGRP expression *in vivo* is analogous to that observed *in vitro*, mFIZZ1 may down-regulate CGRP gene expression during inflammation, decreasing the amount of CGRP available for release from peripheral afferent nerve terminals. Because vascular, inflammatory and airway epithelial cells have been shown to be responsive to CGRP and other neuropeptides (Choi and Kwon, 1998), mFIZZ1, acting through visceral sensory neurons, may modulate one or many of these cell types involved in allergic airway disease.

In summary, a new family of proteins includes at least three murine and two human members. These proteins have distinct tissue-specific expression patterns, and may have distinct biological activity. We characterized *in vitro* the activity associated with mFIZZ1. At concentrations similar to those found *in vivo*, this protein modulates NGF-mediated embryonic DRG survival and gene expression induced by NGF in adult DRG neurons. These activities, together with the expression of FIZZ1 in perineural cells and in inflamed pulmonary epithelium, suggest that mFIZZ1 may mediate interactions between the visceral sensory neurons, inflammatory cells and bronchial tissue in allergic inflammation.

Materials and methods

Animal model of allergic pulmonary inflammation

All animal use was approved by Genentech's Institutional Animal Care and Use Committee. Genentech is accredited by the Association for the Assessment and Accreditation for Laboratory Animal Care International, registered with the United States Department of Agriculture, and follows the *Guide for the Care and Use of Laboratory Animals* (Institute of Laboratory Animal Resources, 1996). To model human allergic pulmonary inflammation, we used the well-characterized mouse model of Renz *et al*. (1992). Six- to eight-week-old female BALB/c mice (Jackson Labs) were sensitized by intraperitoneal injection of 10 μg of OVA (Sigma) plus 1 mg of alum (aluminum hydroxide absorptive medium, 20 mg/ml; Intergren, Purchase, NY). Beginning 2 weeks later, mice were exposed in a closed container for 7 days, 30 min each day, to 10 mg/ml ovalbumin in phosphate-buffered saline (PBS) aerosolized with an UltraNeb nebulizer (DeVilbiss) at a rate of 2 ml/min. Control animals were handled identically, except that no sensitization with OVA preceded the aerosol challenge. Approximately 18 h after the last OVA aerosol challenge, mice were anesthetized, and a cannula connected to one port of a three-way stopcock was inserted into the trachea below the larynx. The lungs were lavaged with three 200 μl aliquots of sterile saline delivered from a syringe attached to the second port of the stopcock. The lungs were gently massaged, and the BALF was withdrawn into a collection syringe attached to the third port of the stopcock. BALF return averaged 80% and did not vary by treatment group. Cellular components of the BALF samples were collected by centrifugation at 1000 *g* for 10 min at 4°C. The supernatants were decanted and frozen individually at –80°C pending further analysis.

Whole-lung tissue samples, obtained from animals with allergic inflammation induced as described above, were homogenized in a Dounce homogenizer containing 10 mM Tris–HCl pH 8.0, 0.14 M NaCl, 0.5% Triton X-100, 1 mM phenylmethyl sulfonyl fluoride (PMSF), 50 μg/ml leupeptin, 1 mM *p*-nitrophenyl phosphate, 50 mM NaF (1.5 ml buffer/100 mg of tissue). The homogenate was allowed to stand for 1 h at 4°C. Insoluble material was collected by centrifugation, and the supernatant was used for western blot analysis.

Protein gel electrophoresis

Aliquots of BALF supernatant (10 μl, containing 0.5–1.0 μg/ml murine serum albumin) were mixed with equal volumes of 2× loading buffer [0.9 M Tris–HCl pH 8.45, 24% v/v glycerol, 0.8% SDS w/v, 0.15% w/v Coomassie Blue G, 0.05% w/v Phenol Red (Novex), supplemented with 2.5% (v/v) β-mercaptoethanol for reducing gels], heat denatured at 85°C for 2 min, resolved on a 16% acrylamide Tricine-buffered gel (Novex), fixed for 30 min in methanol/acetic acid, and silver stained. Separate marker lanes contained Bio-Rad low molecular weight standards or recombinant human interleukin (IL)-8 (8300 Da).

Automated Edman degradation

Electrophoretically resolved proteins were electroblotted onto Millipore Immobilon-P^{sq} polyvinylidene difluoride (PVDF) membranes for 1 h at 250 mA constant current in a Bio-Rad Trans-Blot transfer cell containing 20% methanol in 10 mM 3[cyclohexylamino] 1-propane sulfonic acid (CAPS), 10 mM thioglycolytic acid pH 11 (Matsudaira, 1987). The membrane was stained with 0.1% Coomassie Blue R-250 in 50% methanol for 0.5 min, and destained for 2–3 min with 10% acetic acid in 50% methanol, washed with water and allowed to dry. The band of interest was excised and sequenced by Edman degradation on a PE-Applied Biosystems, Procise 494 HT protein sequencer. The coupling buffer was *N*-methylpiperidine in *N*-propanol and water (25:60:15) supplied by PE-Applied Biosystems. Acetone was routinely added to solvent A to balance the baseline. Peaks were integrated with Justice Innovations software using Nelson Analytical 760 interfaces. Sequence interpretation was performed on a DEC Alpha (Henzel *et al*., 1987).

Nucleotide sequence analysis

To determine the full-length FIZZ1 sequence, the amino acid sequence determined by Edman degradation was used to design degenerate oligonucleotide PCR primers corresponding to the amino acid sequences DETIEI (5′-ACAAACGCGTGAYGARACNATHGARAT-3′) and NPANYP (5′-TGGTGCATGCGGRTARTTNGCNGGRTT-3′). PCR using cDNA reverse-transcribed from normal mouse lung poly(A)$^+$ RNA (Clontech) as the template yielded a 68 bp partial sequence corresponding to nucleotides 105–172 of the final full-length FIZZ1 sequence. Based on these sequence data, an internal primer (5′-ACAAACGCGTGCTGGAGAATAAGGTCAAGG-3′) corresponding to nucleotides 127–144 of the full-length sequence was used in a PCR with oligo(dT) to amplify the 3′ end of the mFIZZ1 sequence. The complete mFIZZ1 sequence was then isolated by screening a normal mouse lung cDNA λ gt10 library (Clontech) with a 50 base end-labeled oligonucleotide probe (5′-ATCTGTTCATAGTCTTGACACTAGTG-CAAGAGAGAGTCTTCGTTACAGTG-3′) corresponding to nucleo-

tides 176–225. Positive phage clones were plaque purified according to standard methods, the inserts were subcloned into Bluescript II SK digested with *Eco*RI, and sequenced according to standard methods.

The nucleotide sequence of murine FIZZ1 was used to conduct BLAST searches (Altschul *et al*., 1990, 1997) of public and private DNA sequence databases. Four homologous sequences were identified. ESTs AA245405 and W42069 contained complete coding sequences for unique murine homologs, designated mFIZZ2 and mFIZZ3, respectively; EST AA524300 contained a complete coding sequence for a human homolog designated hFIZZ1. Another homologous human EST, AA311223, encoded a related sequence designated hFIZZ3. A full-length sequence corresponding to this gene was subsequently identified as follows. mRNA was isolated from human bone marrow using Fast Track 2 reagents and protocols (Invitrogen). Oligo(dT) primed cDNA generated from this RNA was size-selected for product 3–4 kb in length and cloned in the *Xho*I–*Not*I-cleaved pRK5D vector (Life Technologies). Positive clones were identified by screening the resulting library with a [^{32}P]ATP end-labeled oligonucleotide probe (5′-CTTATTGCCCTAAATATTAGG-GAGCCGGCGACCTCCTGGATCCTCTCATT-3′) homologous to the partial cDNA sequence noted above.

Protein sequence homology

The deduced amino acid sequence of the FIZZ family members was analyzed with the Pfam software (HMMER v. 2.1.1; Bateman *et al*., 1999) and Pfam data set 4.0 (May, 1999; 1465 models). Regions of α-helical secondary structure were predicted using the program AGADIR1s-2 (Muoz and Serrano, 1994; Lacroix *et al*., 1998). A three-dimensional fold for mFIZZ1 was sought with the threading program ProCyon (Flöckner *et al*., 1997; King's Beech Software) using a library based on the Brookhaven Protein Data Bank entries of January 15, 1999; the fold library contains 2812 X-ray and NMR structures having <95% sequence identity.

Northern blotting

A 50 base oligonucleotide probe complementary to nucleotides 176–225 of the full-length mFIZZ1 sequence (see above) was end-labeled with [γ-^{32}P]ATP and used to probe a Clontech mouse multiple tissue northern blot using ExpressHyb hybridization solution, as recommended by the manufacturer. The washed blot was exposed to Kodak X-AR film at –70°C. Blots were then stripped and re-probed with a 30-base oligonucleotide complementary to mouse β-actin (Clontech) to assess the quantity of RNA in each lane.

In situ hybridization

PCR primers were designed to amplify 223, 252 and 328 bp fragments of mFIZZ1, mFIZZ2 and mFIZZ3, respectively, in each case including the 5′ untranslated region and most of the coding region. Primers included extensions encoding 27-base T7 or T3 RNA polymerase initiation sites (5′-GGATTCTAATACGACTCACTATATGGGC-3′ and 5′-CTATGA-AATTAACCCTCACTAAAGGGA-3′, respectively) to allow *in vitro* transcription of sense or antisense probes, respectively, from the amplified products. Primers for mFIZZ1 were 5′-T7-CCCAGG-ATGCCAACTTTGA-3′ and 5′-T3-AGGAGGCCCATCTGTTCATAG-3′; primers for mFIZZ2 were 5′-T7-CCCTGAGCTTTCTGGAGAGTG-3′ and 5′-T3-GTGCAGGAGATCGTCTTAGGC-3′; primers for mFIZZ3 were 5′-T7-CGAGGGGGACAGGAGCTAATA-3′ and 5′-T3-GTCCCA-CGAGCCACAGG-3′. Tissues examined by *in situ* hybridization included murine control lung and lung with OVA-induced allergic inflammation, small intestine, large intestine, brain, heart, kidney, liver, mammary gland, skeletal muscle, skin, spleen, stomach, testis and embryos from E12.5 and E15.5. All tissues were fixed in 4% formalin and paraffin-embedded. Sections 5 μm thick were deparaffinized, deproteinated in 4 μg/ml proteinase K for 30 min at 37°C, and further processed for *in situ* hybridization as previously described (Lu and Gillet, 1994). [^{33}P]UTP-labeled sense and antisense probes were hybridized at 55°C overnight, followed by a high stringency wash at 55°C in 0.1× SSC for 2 h. The slides were dipped in NBT2 nuclear track emulsion (Eastman Kodak), exposed in sealed plastic slide boxes containing desiccant for 2–4 weeks at 4°C, developed and counterstained with hematoxylin and eosin.

Generation of anti-FIZZ1 antibody

Rabbit polyclonal antibody to mouse FIZZ1 was generated using the peptide ENKVKELLANPANYP coupled to keyhole limpet hemocyanin. The antigen was injected in complete Freund's adjuvant and boosted every 3 weeks. Post-immune serum samples collected 1 week after each booster dose were pooled and used for western blotting and immunohistochemistry.

Western blotting

BALF samples from inflamed lungs, along with control molecular weight markers (Novex 'Multimark' 4–250 kDa) and purified human IL-8 standard (8.3 kDa), were resolved on Tricine-buffered 16% acrylamide gels (Novex) as described above. Proteins were transferred electrophoretically using an XCell II Blot Module (Novex) in Tris–glycine buffer to PVDF 0.2 μm pore size membranes (Novex). Membranes were blocked overnight at 4°C with 5% non-fat dry milk/0.05% Triton X-100 in PBS, incubated with a 1:1000 dilution of primary antiserum in blocking buffer for 2 h at room temperature (RT). Incubation with a 1:10 000 dilution of peroxidase-conjugated goat anti-rabbit (Cappel) in blocking buffer for 1 h at RT was followed by detection with the ECL kit (Amersham) as recommended by the manufacturer. Parallel membrane strips were incubated with pre-immune serum to confirm the specificity of the post-immune serum.

Immunohistochemistry

Sections (5 μm thick) of formalin-fixed, paraffin-embedded tissue were deparaffinized, and endogenous peroxidase activity was blocked with Kirkegaard and Perry Blocking Solution, diluted 1:10 in water, for 4 min at RT. Samples were deproteinated with 0.4% pepsin in 0.1 N HCl for 10 min at 37°C. All subsequent steps were performed on a Dako Autostainer using reagents diluted in Tris-buffered saline/0.05% Tween-20 (Dako). After blocking non-specific binding with 10% normal goat serum, 1.25 μg/ml rabbit anti-mouse FIZZ1 polyclonal primary antiserum was applied for 1 h at RT. Control slides were incubated with non-immune rabbit immunoglobulin (Zymed). After washing, a 1:200 dilution of secondary goat anti-rabbit biotinylated IgG antibody (Vector Labs) was applied for 30 min at RT. Biotinylated antibody was detected using Vector Labs Standard ABC Elite kit reagents, followed by incubation with Pierce metal-enhanced diaminobenzidine, according to manufacturers' protocols. To delineate further the discrete cells expressing mFIZZ1 in neurovascular bundles in lung peribronchial stroma and the large bowel, serial sections of these tissues were stained as described above for mFIZZ1 and with anti-PGP9.5 (Chemicon AB1761), anti-NSE (Chemicon AB951) and anti-S-100 (Dako Z0628).

Production and purification of murine FIZZ proteins

The full-length mFIZZ1 insert was cloned in pST31, which encodes a polyhistidine sequence, and was expressed in *Escherichia coli.* Bacterial cells were dissolved (5% w/v) in 0.1 M Tris pH 9.0, 7.0 M guanidine. Sulfhydryl groups were blocked with 0.1 M sodium sulfite, 20 mM sodium tetrathionate, and the supernatant was filtered through a 0.45 μm pore membrane. The crude cell lysates were applied to NTA affinity resin in 25 mM Tris pH 7.5, 20 mM glycine, 6 M urea, the column was washed with the same buffer containing 50 mM imidazole, and the FIZZ protein was then eluted in the same buffer containing 250 mM imidazole. Eluted protein was diluted to 0.1 mg/ml in 0.1 M Tris, 20 mM glycine, 0.3 M NaCl, 5 mM EDTA, 2 M urea, adjusted to pH 8.6, and then made 5 mM in cysteine. The sample was allowed to refold overnight at 4°C. Refolded monomeric protein was purified by preparative HPLC on a C4 column in 0.05% trifluoroacetic acid, 10% acetonitrile eluted with a 35–55% acetonitrile gradient. Purified fractions were dialyzed into 30 mM acetate, 150 mM NaCl pH 4.8.

Dorsal root ganglion cultures

For embryonic cultures, DRG were harvested from all axial levels of E14 rat embryos, dissociated with trypsin and plated at 500 neurons per well in polyornithine-coated 384-well plates in F12 medium with serum-free supplements as described (Davies *et al*., 1993). Test compounds were added at the time of plating. Surviving neurons were counted after 3 days of culture.

Adult rat DRG cultures were prepared essentially as described (Lindsay *et al*., 1989). They were grown for 7 days in polyornithine/laminin-coated 24 well plates in serum-free media as above, with the addition of NGF and/or FIZZ protein at the time of plating. CGRP expression was measured by immunocytochemistry. The cultures were fixed for 1 h on ice with 4% paraformaldehyde, 15% saturated picric acid, in 0.1 M phosphate buffer pH 7.4, washed five times in TBST (0.125 M NaCl, 25 mM Tris pH 7.4, 0.1% Triton X-100) and then blocked in 5% goat serum in TBST. The cultures were stained with antibodies to NeuN (Mullen *et al*., 1992), a marker of neuronal nuclei, and CGRP (Sigma C8198, rabbit anti-rat polyclonal) in TBST with 1% goat serum overnight. They were washed again and then incubated with secondary

antibodies labeled with Cy3 or BODIPY, washed and viewed with a Nikon inverted fluorescence microscope. All counting and image capturing was performed in a blind fashion. Entire wells were scanned and neurons were identified by positive staining with NeuN. Independent measurements were then made of the number of CGRP-positive neurons, and the brightness of those neurons was determined using NIH Image software for densitometric analysis of CGRP staining.

NGF binding to trkA–IgG was performed as described (Shelton *et al*., 1995).

SPR biosensor assays

A BIAcore-2000™ SPR system (BIAcore, Inc., Piscataway, NJ; Lofas and Johnsson, 1990) was used to assess possible binding interactions between the proteins mFIZZ1, NGF and trkA–IgG. A carboxymethyl dextran (CM5) biosensor chip was activated with *N*-ethyl-*N*′-(3-dimethylaminopropyl)-carbodiimide hydrochloride and *N*-hydroxy-succinimide according to the manufacturer's instructions. Thereafter, mFIZZ1, NGF, trkA–IgG, or an unrelated IgG (Herceptin™; Genentech, Inc.), each in 10 mM sodium acetate pH 4.8, was injected for coupling, yielding surface densities of ~2900, 120, 1500 and 1400 response units, respectively. Finally, 1 M ethanolamine was injected to block unreacted groups on the dextran.

For binding experiments, mFIZZ1, NGF and trkA–IgG were diluted to 0.1 mg/ml in running buffer (PBS containing 0.05% Tween-20) and injected at 25°C using a flow rate of 10 µl/min. Regeneration was achieved with 10 mM HCl. Net binding was assessed by subtracting the signal observed on the unrelated IgG surface from that observed on each test surface.

Acknowledgements

We wish to acknowledge the contribution of the following people: Jeff Tepper for assistance with the BAL technique; Alane Gray and Bill Woods for guidance in the initial cloning of murine FIZZ1; Audrey Goddard and the DNA sequencing laboratory for the sequence of the full-length murine FIZZ1 clone; Dick Vandlen for help with purification of murine FIZZ1; the Oligonucleotide and Peptide Synthesis laboratories; Greg Bennet for generation of the anti-mFIZZ1 antiserum; Thuy Nguyen for initial *in situ* hybridizations; Patti Tobin and Robin Taylor in the Anatomic Pathology laboratory for preparation of tissue sections.

References

Altschul,S.F., Gish,W., Miller,W., Myers,E.W. and Lipman,D.J. (1990) Basic local alignment search tool. *J. Mol. Biol.*, **215**, 403–410.

Altschul,S.F., Madden,T.L., Schaffer,A.A., Zhang,J., Zhang,Z., Miller,W. and Lipman,D.J. (1997) Gapped BLAST and PSI-BLAST: a new generation of protein database search programs. *Nucleic Acids Res.*, **25**, 3389–3402.

Barnes,P.J. (1996) Neuroeffector mechanisms: the interface between inflammation and neuronal responses. *J. Allergy Clin. Immunol.*, **98**, S73–S81.

Bateman,A., Birney,E., Durbin,R., Eddy,S.R., Finn,R.D. and Sonnhammer,E.L.L. (1999) Pfam 3.1: 1313 multiple alignments and profile HMMs match the majority of proteins. *Nucleic Acids Res.*, **27**, 260–262.

Blyth,D.I., Pedrick,M.S., Savage,T.J., Hessel,E.M. and Fattah,D. (1996) Lung inflammation and epithelial changes in a murine model of atopic asthma. *Am. J. Respir. Cell Mol. Biol.*, **14**, 425–438.

Bonini,S., Lambiase,A., Bonini,S., Angelucci,F., Magrini,L., Manni,L. and Aloe,L. (1996) Circulating nerve growth factor levels are increased in humans with allergic diseases and asthma. *Proc. Natl Acad. Sci. USA*, **93**, 10955–10960.

Braun,A., Appel,E., Baruch,R., Herz,U., Botchkarev,V., Paus,R., Brodie,C. and Renz,H. (1998) Role of nerve growth factor in a mouse model of allergic airway inflammation and asthma *Eur. J. Immunol.*, **28**, 3240–3251.

Choi,D.-C. and Kwon,O.-J. (1998) Neuropeptides and asthma. *Curr. Opin. Pulm. Med.*, **4**, 16–24.

Davies,A.M., Horton,A., Burton,L.E., Schmelzer,C., Vandlen,R. and Rosenthal,A. (1993) Neurotrophin-4/5 is a mammalian-specific survival factor for distinct populations of sensory neurons. *J. Neurosci.*, **13**, 4961–4967.

Flöckner,H., Domingues,F.S. and Sippl,M.J. (1997) Protein folds from pair interactions: a blind test in fold recognition. *Proteins (Suppl.)*, **1**, 129–133.

Henzel,W.J., Rodriquez,H. and Watanabe,C. (1987) Computer analysis of automated Edman degradation and amino acid data. *J. Chromatogr.*, **404**, 41–52.

Horton,A.R., Barlett,P.F., Pennica,D. and Davies,A.M. (1998) Cytokines promote the survival of mouse cranial sensory neurones at different development stages. *Eur. J. Neurosci.*, **10**, 673–679.

Institute of Laboratory Animal Resources (1996) *Guide for the Care and Use of Laboratory Animals*. National Research Council, National Academy of Sciences, National Academy Press, Washington, DC.

Lacroix,E., Viguera,A.R. and Serrano,L. (1998) Elucidating the folding problem of α-helices: Local motifs, long-range electrostatics, ionic-strength dependence and prediction of NMR parameters. *J. Mol. Biol.*, **284**, 173–191.

Levi-Montalcini,R. and Angeletti,P.U. (1963) Essential role of nerve growth factor in the survival and maintenance of dissociated sensory and sympathetic nerve cells *in vitro*. *Dev. Biol.*, **7**, 653–659.

Lindsay,R.M. and Harmar,A.J. (1989) Nerve growth factor regulates expression of neuropeptide genes in adult sensory neurons. *Nature*, **337**, 362–364.

Lindsay,R.M., Lockett,C., Sternberg,J. and Winter,J. (1989) Neuropeptide expression in cultures of adult sensory neurons: modulation of substance P and calcitonin gene-related peptide levels by nerve growth factor. *Neuroscience*, **33**, 53–65.

Lofas,S. and Johnsson,B. (1990) A novel hydrogel matrix on gold surfaces in surface plasmon resonance sensors for fast and efficient covalent immobilization of ligands. *J. Chem. Soc. Commun.*, **21**, 1526–1528.

Lu,L.H. and Gillett,N.A. (1994) An optimized protocol for *in situ* hybridization using PCR generated ^{33}P-labeled riboprobes. *Cell Vision*, **1**, 169–176.

Matsudaira,P. (1987) Sequence from picomole quantities of proteins electroblotted onto polyvinylidene difluoride membranes. *J. Biol. Chem.*, **262**, 10035–10038.

McFadden,E.R.,Jr and Gilbert,I.A. (1992) Asthma. *N. Engl. J. Med.*, **327**, 1928–1937.

Mullen,R.J., Buck,C.R. and Smith,A.M. (1992) NeuN, a neuronal specific nuclear protein in vertebrates. *Development*, **116**, 201–211.

Muoz,V. and Serrano,L. (1994) Elucidating the folding problem of helical peptides using empirical parameters. *Nature Struct. Biol.*, **1**, 399–409.

Petersen,M., Segond von Banchet,G., Heppelmann,B. and Koltzenburg,M. (1998) Nerve growth factor regulates the expression of bradykinin binding sites on adult sensory neurons via the neurotrophin receptor p75. *Neuroscience*, **83**, 161–168.

Renz,H., Smith,H.R., Henson,J.E., Ray,B.S., Irvin,C.G. and Gelfand,E.W. (1992) Aerosolized antigen exposure without adjuvant causes increased IgE production and increased airway responsiveness in the mouse. *J. Allergy Clin. Immunol.*, **89**, 1127–1138.

Shelton,D.L., Sutherland,J., Gripp,J., Camerato,T., Armanini,M.P., Phillips,H.S., Carroll,K., Spencer,S.D. and Levinson,A.D. (1995) Human trks: molecular cloning, tissue distribution and expression of extracellular domain immunoadhesins. *J. Neurosci.*, **15**, 477–491.

Shu,X.Q. and Mendell,L.M. (1999) Neurotrophins and hyperalgesia. *Proc. Natl Acad. Sci. USA*, **96**, 7693–7696.

Spina,D., Shah,S. and Harrison,S. (1998) Modulation of sensory nerve function in the airways. *Trends Pharmacol. Sci.*, **19**, 460–466.

Received November 24, 1999; revised May 24, 2000; accepted June 7, 2000